Journal of Technology Research (JTR)
Volume 3, Special Issue, (2025), pp 282-289, ISSN 3005-639X
The 7th Conference of Engineering Sciences and Technology (CEST-2025)

# Axial Compression Behavior of Locally Corroded Slender Circular CFST Columns: An Experimental Study

Faesal Alatshan[1*], Siti Aminah Osman[2], Roszilah A. Hamid[2]

[1] Civil Engineering Department, College of Engineering Technology, Houn, Libya.

[2] Department of Civil Engineering, Faculty of Engineering and Built Environment, Universiti Kebangsaan Malaysia, Selangor, Malaysia.

*Corresponding author email: f.alatshan@ceh.edu.ly

Received: 30-09-2025 | Accepted: 25-11-2025 | Available online: 25-12-2025 | DOI:10.26629/jtr.2025.29

**ABSTRACT**

This study presents an experimental investigation into the axial compression behavior of slender circular concrete-filled steel tube (CFST) columns affected by localized corrosion. While CFST systems are known for their structural efficiency and durability, their performance under corrosion-induced damage—particularly in marine environments—remains insufficiently understood, especially for slender columns. Two full-scale CFST specimens were prepared: a control column and a corroded column with a mid-height defect induced through an electrochemical technique simulating localized marine corrosion. Both specimens were tested under axial compression with pin-ended boundary conditions. The results indicate that localized corrosion significantly alters failure modes, reduces load-carrying capacity, and compromises structural stability. The corroded specimen exhibited a 12% reduction in ultimate strength and experienced sudden failure, highlighting the vulnerability of slender CFST columns to corrosion-induced instability. The results provide preliminary insights into the combined effects of wall-thinning and reduced confinement in slender CFSTs, and serve as a basis for future research aiming to enhance the understanding of corrosion-damaged CFST structures.

**Keywords:** Concrete-Filled Steel Tubes (CFSTs); Localized Corrosion; Slender Columns; Experimental Study; Composite Structures.

# سلوك الضغط المحوري لأعمدة CFST الدائرية النحيلة المتآكلة محليًا دراسة تجريبية

فيصل العطشان[1*]، سيتي أمينة عثمان[2]، روزيلاه أ. حميد[2]

[1]قسم الهندسة المدنية، كلية تقنية الهندسة، هون، ليبيا.

[2] قسم الهندسة المدنية، كلية الهندسة والبيئة المبنية، الجامعة الوطنية الماليزية (UKM) ، سلانغور ماليزيا

**ملخـــــص البحـــــث**

يقدّم هذا البحث دراسة تجريبية لسلوك الأعمدة الدائرية النحيفة المملوءة بالخرسانة والمغلفة بالحديد (**CFST**) عند تعرضها للتآكل الموضعي تحت تأثير الضغط المحوري. ورغم ما تتميز به أنظمة **CFST** من كفاءة إنشائية ومتانة عالية، إلا أنّ أدائها عند التعرض لتلف ناتج عن التآكل، خصوصًا في البيئات البحرية، ما يزال غير مفهوم بشكل كافٍ، لا سيما في حالة الأعمدة النحيفة. تم تجهيز عيّنتين بالحجم الحقيقي الكامل: العمود الأول ضُبط كعينة مرجعية (سليمة)، بينما جُهّز العمود الثاني بتأكل موضعي عند منتصف الارتفاع باستخدام تقنية كهروكيميائية لمحاكاة التآكل البحري الموضعي. خضعت العيّنتان لاختبار ضغط محوري مباشر ضمن شروط

ارتكاز مفصلية. أظهرت النتائج أنّ التآكل الموضعي يُغيّر أنماط الفشل بشكل ملحوظ، ويُقلّل من القدرة التحميلية، ويُضعف الاستقرار الإنشائي. حيث سجّل العمود المتآكل انخفاضًا بنسبة 12% في المقاومة النهائية، وحدث له انهيار مفاجئ، ممّا يبرز هشاشة الأعمدة النحيفة **CFST** تجاه عدم الاستقرار الناتج عن التآكل. توفر النتائج رؤى أولية حول التأثيرات المشتركة لترقيق الجدار وتقليل الاحتجاز في أنابيب الصلب المملوءة بالخرسانة **(CFSTs)** النحيلة، وتعمل كأساس للبحوث المستقبلية التي تهدف إلى تعزيز فهم هياكل أنابيب الحديد المملوءة بالخرسانة **(CFSTs)** التالفة بسبب التآكل.

**الكلمات المفتاحية:** أنابيب الصلب المملوءة بالخرسانة **(CFSTs)**؛ التآكل الموضعي؛ الأعمدة النحيلة؛ الدراسة التجريبية؛ الهياكل المركبة.

## 1. INTRODUCTION

Concrete-filled steel tubes (CFSTs) have been used in structural engineering for over a century [1-3]. highlighting the need to study their durability and long-term performance. Since detailed research began in the 1960s, CFSTs have proven superior to traditional systems like HSS and RC by combining the strengths of steel and concrete. This synergy improves strength, ductility, seismic resistance, and fire performance, while enabling smaller cross-sections, eliminating formwork, and reducing construction costs. [4, 5].

Corrosion of the steel tube is a major durability concern for CFST members, particularly in humid or chloride-rich environments. Localized corrosion (pitting) can reduce the steel wall thickness and weaken the confinement effect on the concrete core, leading to a reduction in axial strength and stiffness.

Limited research efforts have been previously made to investigate the effect of localized corrosion on CFSTs. Recent study by Alatshan et al. [6] examined the residual compressive strength of locally corroded circular CFST stub columns. The results showed that corrosion significantly affects failure modes, load-strain relationships, and ultimate compressive capacities. The study concluded that localized corrosion reduces the load-carrying capacity and durability of CFST columns, but mechanical damage can approximate actual corrosion effects, offering insights into the structural behavior of damaged columns. Following this, Fang et al. [7] experimentally and numerically demonstrated that, among the three dimensions of a local corrosion zone (radial depth, annular width, axial length) of CFST stub columns, the radial corrosion depth has the most pronounced effect on bearing capacity, and they proposed a practical formula to estimate residual strength from geometric measurements of corrosion .

Furthermore, eccentrically loaded CFST members with localized corrosion have been studied by Lin et al. [8] and Luo et al. [9], revealing that corrosion position, depth ratio, and loading eccentricity jointly govern capacity loss in both stub and long columns, and enabling the development of design models for practical assessment . More recently, Li et al. [10] investigated slender CFST columns with randomly distributed pitting corrosion, introducing a controlling-section approach to reliably predict ultimate strength under variable pit distributions.

However, design codes still provide limited guidance for evaluating the residual strength of corroded CFST columns, particularly slender ones. More experimental evidence on electrochemically corroded slender CFSTs is needed to support durability-based assessment and design.

Although previous studies have partly enhanced the understanding of corrosion effects on CFSTs, knowledge regarding slender CFST columns subjected to localized electrochemical corrosion remains limited. Most prior research has either exclusively focused on short (stub) columns or employed artificial methods, such as

mechanically machined grooves or drilled pits, to simulate corrosion in slender columns. Such artificial approaches may not accurately capture the complexities of actual, time-dependent electrochemical corrosion processes. Therefore, this study aims to bridge this research gap by experimentally investigating the effects of localized electrochemical corrosion on the axial compressive behavior of slender circular CFST columns.

## 2. Experimental program

Two circular CFST slender columns were prepared and tested under axial compression loading. Of which one intact specimen was used as a control sample, while the other column was locally corroded at its mid-height. The corrosion was applied using the electrochemical approach. The specimens' details are illustrated in Table 1 and Figure 1. As shown, the specimens had the same dimensions with a height of 2m, an external diameter of 114mm, and a thickness of 3.2mm.

Generally, the selected circular tube sizes utilized in the columns have a diameter to thickness ratio (*D/t*) of 35 and a height to diameter ratio (*H/D*) of 17, which are in line with the values adopted by the previous investigation conducted on CFST long columns [11, 12]. Additionally, the columns can be classified as slender columns as suggested by the European standard [13], in which the *H/D* ratio should be more than 4.


**Fig 2**. Steel tensile coupon test.

**Table 1.** Dimensions of the Specimens.

| No. | Specimen | Corrosion depth | Corrosion Height |
|---|---|---|---|
| | | $t_c$ (mm) | $H_c$ (mm) |
| 1 | G3-tc0-hc0 | 0 | 0 |
| 2 | G3-tc1.2-hc200 | 1.2 | 200 |

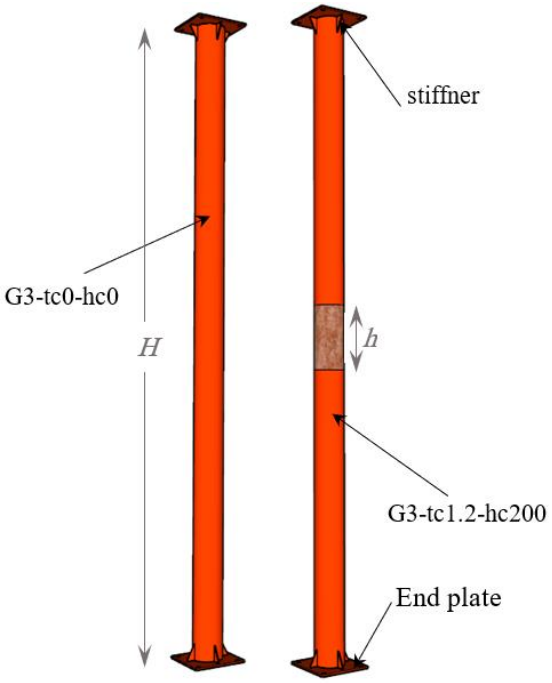


**Fig 1.** specimens' details.

The average modulus of elasticity (*Es*) and the yield strength ($f_y$) of the steel tubes were measured using tensile coupon tests. As illustrated in Figure 2, steel coupons were cut from the tubes according to ASTM-E8/E8M [14]. These coupons were subjected to axial tensile loadings on a Universal Testing Machine with a capacity of 100KN (Figure 2). The resulting stress-strain curves of the steel are presented in Figure 3. Additionally, Table 2 shows the average results from the steel coupon testing. As illustrated, the average test yield strengths of the steel were measured as 292 MPa.

**Table 2**: The measured properties of the steel tubes.

| $f_y$ (MPa) | $\varepsilon_y$ (%) | $f_u$ (MPa) | $\varepsilon_u$ (%) | $E_s$ (GPa) | $\varepsilon_r$ (%) |
|---|---|---|---|---|---|
| 292 | 0.53 | 340 | 12.23 | 190 | 27.30 |

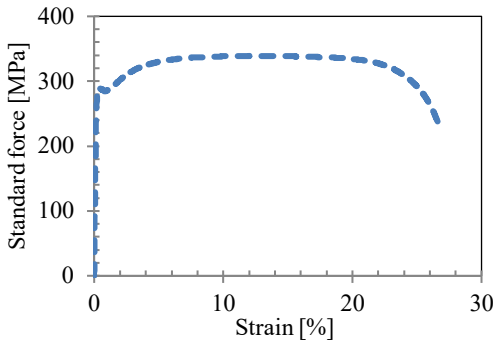


**Fig 3**. Stress-strain relationships of the steel tubes.

### *2.1 Concrete properties*

The concrete was designed following ACI:211 [15] and used to fill steel tubes. Ordinary Portland cement (ASTM: type I), silica river sand, and limestone gravel (max size 10 mm) were used, with tap water for mixing. The concrete was poured into steel tubes, covered with plastic sheets to minimize evaporation, and cured in laboratory conditions.

150 mm concrete cubes were cast, demolded after 24 hours, and cured in water for 28 days. The compressive strength ($f_{cu}$) of the mixtures, determined according to BS-1881-116 [16], averaged 25 MPa after 28 days.

### *2.2 Specimens' preparation*

Steel tubes were cut to the specified column heights using an electric saw and sealed with welded end plates to prevent leakage during casting. After surface cleaning, concrete was poured in layers and compacted using an electric vibrator to eliminate voids and ensure uniformity.

### *2.3 Corrosion process*

Following casting and curing, corrosion was induced using the impressed current technique to simulate localized marine corrosion, as illustrated in Figure 4. The steel tubes were first abraded to remove the protective paint layer, and a DC power supply was employed, connecting the positive terminal to the steel tube (anode) and the negative to a copper rod (cathode), both immersed in a 3.5% NaCl solution. A constant current of 2.0 A was applied to accelerate the corrosion process. The initial exposure duration was estimated using Faraday's law, expressed as:

$$T(s) = \frac{m_{loss}\, F\, Z_{Fe}}{I\, M_{Fe}}$$

In which $m_{loss}$ is the mass of the corroded steel (g), F is the Faraday's constant equal to 96,500 C.mol-1, $Z_{Fe}$ is the ionic charge equal to 2 for Fe2+, I is the imposed current density (A) and $M_{Fe}$ is the atomic weight of iron equal to 56g/mol.

This theoretical calculation provided a preliminary estimate of the required exposure time to achieve a target corrosion depth of approximately 1.2 mm. However, the final duration was refined experimentally based on periodic wall-thickness measurements using a digital caliper to ensure the actual corrosion depth matched the intended value.

The solution's pH was monitored and replaced every 2–3 days to ensure stability. Tube thickness reduction was regularly measured, and the process continued until the desired corrosion rates were reached. Corroded surfaces were then cleaned using a sandpaper wheel to facilitate bonding with repair materials. Final corrosion levels were quantified via outer diameter measurements using a digital caliper.

### *2.4 Compression Test Setup*

The columns were tested using multipurpose loading frame systems at the Concrete and

Materials Laboratory at Universiti Kebangsaan Malaysia (UKM). As shown in Figure 5, the loading frame consists of four steel columns and three girders. An actuator having a maximum capacity of 1000 KN and with a displacement loading control system was utilized. The applied load was measured using a load cell attached to the top girders. The details of the test instrumentation and setup of long columns are illustrated in Figure 6**Error! Reference source not found.**.

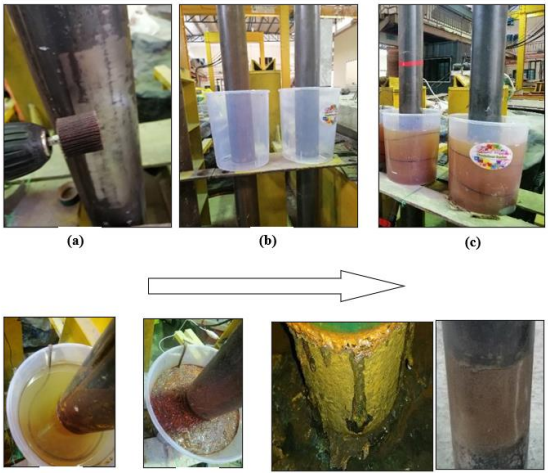


**Fig. 4:** Steps before and through the corrosion process of long columns: (a) Intact specimen (b) Removing the protective layer, (b) Side view before corrosion, (c) Side view after corrosion, (d) Top view before corrosion, (c) Top view after corrosion, (d) the defective column.


**Fig. 5.** The utilized loading frame systems to test the long CFST columns.

Hinge-hinge boundary conditions were adopted using the built-in top swivels and the fabricated pin support using cylindrical rollers at the bottom of the columns. The supports shown in Figure 7 were to simulate pinned-end circumstances by allowing free rotations around the main axis while restricting rotations around the orthogonal axis. In addition, two end plates with four vertical stiffeners were welded to the top and bottom of the columns. Five LVDTs were mounted on the side of the specimens to measure the horizontal displacement at equally spaced positions, along with the height of the specimens during the loading process. In addition, two strain gauges were attached to the mid-height of the long columns in both the axial and the lateral directions

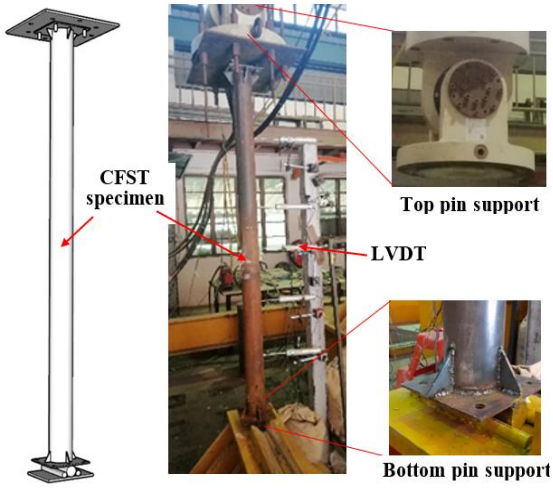


**Fig 6.** Test setup of the CFST Long columns.

After installing the columns at the loading frame, a slight preload was applied to the specimens and then unloaded to guarantee the mechanical alignment of the columns. Then, the compression load was applied to the columns until complete failure.

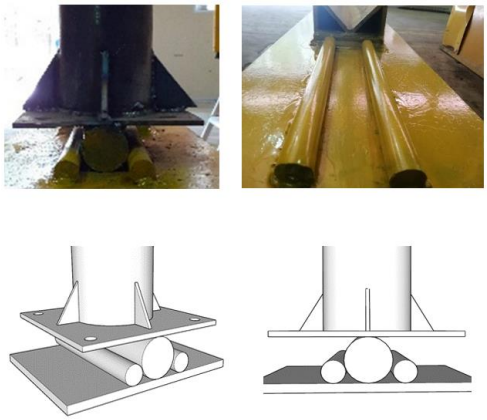

**Fig 7**. Fabrication of the bottom hinge support of the long columns.

## 3. Results and Discussion

### *3.1 Corrosion results*

This section outlines the longitudinal corrosion patterns observed after subjecting the specimens to controlled corrosion conditions. The extent of corrosion was quantified by measuring the external diameter of the steel tubes using a digital caliper. As depicted in Figure 8, the resulting profiles demonstrate variations in corrosion height and depth, aligned with the intended parameters of the experimental setup.

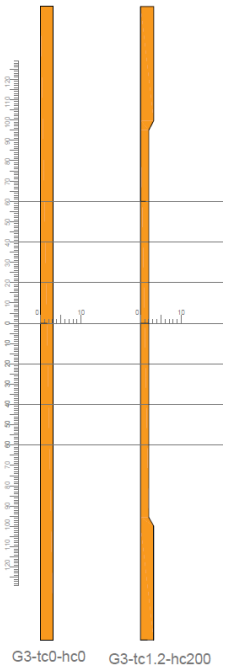


**Fig 8**. Longitudinal sections of the corroded area at the mid-height of G3 specimens.

### *3.2 FAILURE MODES*

As can be deduced, the two CFST columns failed at their mid-heights and were governed by global buckling that followed the shape half-sine wave, which is expected for such pinned-ended columns. In addition, no inward buckling was observed due to the support of the steel tube by the concrete infill.

Figure 9 presents a comparison between the failure pattern at the mid-heights of the intact (G3-tc0-hc0) and corroded (G3-tc1.2-hc200) CFST long columns. As can be seen, the failure modes could be significantly affected by the presence of the corrosion, where the corrosion led to more severe buckling compared to the control intact specimen. Attention can be paid to the fact that localized corrosion can alter the mechanism of load-transferring and the composite interaction, which can change the failure mode simultaneously.

In detail, this difference in failure modes can be mainly attributed to the reduced wall thickness of the steel tube, resulting in a reduction in the cross-sectional capacity, as well as a weakening of the confinement strength provided by the steel tube to the concrete core.

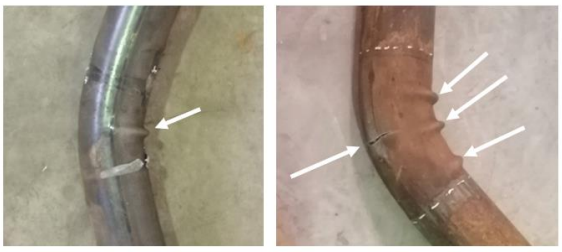


**Fig 9**. The impact of localized corrosion on the failure mode of long CFST columns

### *3.3 Axial load- strain relationships*

Figure 10 illustrates the typical outcomes obtained from the compression testing of CFST long slender columns. In the figure, the applied axial load is plotted against the measured axial

strain. For both the intact and corroded columns, linear elastic behaviour is observed until reaching their ultimate capacity of 476 KN and 418 KN, respectively.

Just after that, and for the intact column (G3-tc0-hc0) the load resistance gradually declined with deflection increase. However, a sudden failure occurred for the corroded specimen (G3-tc1.2-hc200) after reaching its peak load. Sudden failure is expected for slender or long columns and occurs due to lateral instability phenomena [17]. In other words, the long, centrally-loaded column remains stable until a critical load is reached, as the lateral displacement increases uncontrollably rapidly with a relatively small increase in axial resistance, which bends at the weaker side of the bearing shaft. Sudden collapse can be more critical for corroded columns, as the limited thickness of the steel tube cannot effectively resist the concrete core's tendency to brittle failure.

The corroded specimen has an ultimate strength reduction of 12% as compared to the intact specimens. This decline in the mechanical properties is attributed to the reduction in the wall thickness of the steel tube, which reduces direct resistance provided by the steel, in addition to the reduction of the confinement effect on concrete infill.

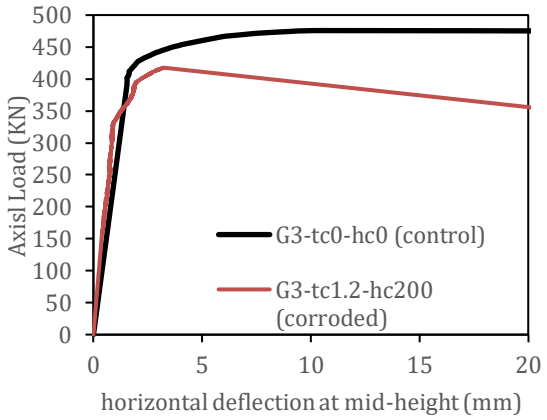


**Fig 10**. Axial load- horizontal deflection relationships of CFST specimens in G3.

## 4. Conclusion

This study experimentally investigated the axial compression behavior of slender circular CFST columns subjected to localized corrosion. Two full-scale specimens were tested, including an intact column and another with a mid-height corrosion defect. The findings reveal that localized corrosion significantly affects the structural performance of CFST columns. Specifically, the corroded specimen exhibited a 12% reduction in ultimate load capacity and a more sudden failure mode compared to the intact specimen. This performance degradation is primarily attributed to the reduced steel wall thickness, which compromises both the axial strength and the confinement provided to the concrete core. The results also confirm that slender CFST columns are particularly vulnerable to instability under axial loading when corrosion is present, emphasising the need for durability considerations in marine and aggressive environments.

Given the limited sample size (one specimen per condition), the outcomes of this work should be regarded as exploratory and serve as a preliminary step toward broader experimental and analytical research on corrosion-damaged CFST columns.

## References

[1] Mahlouji J. Analysis of steel-reinforced concrete-filled steel tubular and concrete-filled steel tubular columns under cyclic loading. Johor: Universiti Teknologi Malaysia, Faculty of Civil Engineering; 2013.

[2] Li L, Lei K. Preliminary design and cross-sectional form study of closed-type concrete-filled steel tube support for traffic tunnel. Symmetry. 2020;12(8):1368. Available from: https://www.mdpi.com/2073-8994/12/8/1368

[3] Qian J, Li N, Ji X, Zhao Z. Experimental study on the seismic behavior of high strength concrete filled double-tube columns. Earthquake Eng Eng Vib. 2014;13(1):47–57.

[4] Zhao X-L, Han L-H, Lu H. Concrete-filled tubular members and connections. London: CRC Press; 2010.

[5] Kodur VKR. Performance-based fire resistance design of concrete-filled steel columns. J Constr Steel Res. 1999;51(1):21–36. doi: 10.1016/S0143-974X(99)00003-6.

[6] Alatshan F, Osman SA, Hamid RA, Mashiri F. Residual compressive strength of locally corroded circular CFST stub columns: An experimental study. IOP Conf Ser Earth Environ Sci. 2024;1369(1):012036. doi: 10.1088/1755-1315/1369/1/012036.

[7] Fang W, Chen M, Wen Q, Huang H, Xu K, Zhang R. Experimental and numerical investigation on the bearing capacity of axially compressive concrete-filled steel tubular columns with local corrosion. Buildings. 2024;14(11):3628. Available from: https://www.mdpi.com/2075-5309/14/11/3628

[8] Lin S, Li Z, Zhao Y-G. Behavior of eccentrically loaded circular concrete-filled steel tube stub columns with localized corrosion. Eng Struct. 2023;288:116227. doi: 10.1016/j.engstruct.2023.116227.

[9] Luo S, Chen M, Huang H, Xv K, Fang W, Zhang R. Eccentric compression test and ultimate load strength analysis of circular CFST long column with local corrosion. Structures. 2023;56:104937. doi: 10.1016/j.istruc.2023.104937.

[10] Li J, Jia C, Gao S, Guo L. Experimental and numerical study on axial compression behavior of slender CFST columns with localized pitting corrosion damage. Constr Build Mater. 2024;414:134858. doi: 10.1016/j.conbuildmat.2023.134858.

[11] Masuo K, Adachi M, Kawabata K, Kobayashi M, Konishi M. Buckling behavior of concrete filled circular steel tubular columns using lightweight concrete. In: Wakabayashi M, editor. Proc Third Int Conf Steel-Concrete Composite Structures; 1991 Sep; p. 26–29.

[12] Ghannam S, Jawad YA, Hunaiti Y. Failure of lightweight aggregate concrete-filled steel tubular columns. Steel Compos Struct. 2004;4(1):1–8.

[13] European Committee for Standardization (CEN). Design of composite steel and concrete structures – Part 2: General rules and rules for bridges (EN 1994-2). Brussels: CEN; 1994.

[14] ASTM International. Standard test methods for tension testing of metallic materials. ASTM E8/E8M. West Conshohocken (PA): ASTM; 2013.

[15] American Concrete Institute (ACI). Standard practice for selecting proportions for normal, heavyweight, and mass concrete. ACI 211; 1991.

[16] British Standards Institution (BSI). Methods of testing concrete: Method for determination of compressive strength of concrete cubes. BS 1881-116. London: BSI; 1983.

**[17]** Hailemichael K, Liivo B. Stability of slender columns. Master's Thesis. Lund: Division of Structural Engineering, Lund University; 2014